Available online at www.sciencedirect.com
SCIENCE DIRECT®
Spectrochimica Acta Part A xxx (2006) xxx–xxx
SPECTROCHIMICA ACTA PART A
www.elsevier.com/locate/saa

Sub-ppm multi-gas photoacoustic sensor

Jean-Philippe Besson *, Stéphane Schilt, Luc Thévenaz

Ecole Polytechnique Fédérale de Lausanne (EPFL), Laboratory of Nanophotonics and Metrology (NAM), CH-1015 Lausanne, Switzerland

Received 16 September 2005; received in revised form 2 October 2005; accepted 17 October 2005

Abstract

A photoacoustic multi-gas sensor using tuneable laser diodes in the near-infrared region is reported. An optimized resonant configuration based on an acoustic longitudinal mode is described. Automatic tracking of the acoustic resonance frequency using a piezo-electric transducer and a servo electronics is demonstrated. Water vapour, methane and hydrogen chloride have been measured at sub-ppm level in different buffer gas mixtures. The importance of the system calibration in presence of several diluting gases is discussed. Finally, trace gas measurements have been assessed and detection limits (signal-to-noise ratio = 3) of 80 ppb at 1651.0 nm for CH_4, 24 ppb at 1368.6 nm for H_2O and 30 ppb at 1737.9 for HCl have been demonstrated.

Keywords: Photoacoustic spectroscopy; Multi-gas sensing; Trace gas detection; DFB lasers

1. Introduction

Photoacoustic spectroscopy (PAS) is a well-established technique for measurements of trace gases at atmospheric pressure in various applications, such as environmental monitoring [1], industrial process control [2] or medical diagnostic by breath analysis [3]. PAS is a calorimetric method in which the optical energy absorbed in a gas sample is directly measured through the thermal transfer induced in the medium. The conversion from optical energy to heat is produced by molecular absorption of photons of proper wavelength and subsequent non-radiative relaxation of the excited vibrational state (collisional relaxation). When the deposited optical energy is modulated, a periodic heating is produced, generating also a modulation of the sample pressure. This constitutes an acoustic wave, which can be detected using a sensitive microphone. This technique provides many advantages in terms of sensitivity (ppm to ppb detection limits) and selectivity, when used in connection with single frequency laser diodes. Furthermore, multi-gas detection, real-time measurements, continuous monitoring and an excellent linearity over several orders of magnitude are achievable. However, the photoacoustic (PA) signal is directly proportional to the incident laser power, which is typically a few tens of milliwatt only for standard distributed feedback (DFB) laser diodes dedicated to optical telecommunication. The use of a properly designed resonant configuration decreases the importance of this limitation by improving the sensitivity.

Standard telecommunication laser diodes are commonly used in compact PA sensors in the NIR due to their modulation capabilities (frequency or intensity modulation through modulation of the injection current), their high reliability and their spectral characteristics. In addition, they are tuneable over a few nanometers, which allow a perfect matching between the emission line of the laser and the centre of the investigated absorption line. The compatibility with optical fibres is also a key issue for multi-gas monitoring as it facilitates the alignment of the whole system.

Multi-gas monitoring is required for process control in the manufacturing of the novel low-water-peak fibres developed for optical telecommunications. This new type of fibres is designed to enable optical transmission in the E-band (1360–1460 nm) in order to open up this window for implementing cost-effective coarse wavelength division multiplexing (CWDM) technology for current or future network applications [4]. The presence of hydrogenated compounds like H_2O, HCl and CH_4 during the fabrication of these fibres dramatically impairs the performances of the end-product as they contribute to a strong OH^- absorption peak centred at 1390 nm. Therefore, these species need to be monitored at sub-ppm level during the manufacturing process of the silica perform, which is based on the modified chemical vapour deposition process. This manufacturing must

* Corresponding author.
E-mail address: Jean-Philippe.Besson@epfl.ch (J.-P. Besson).

1386-1425/$ – see front matter © 2005 Elsevier B.V. All rights reserved.
doi:10.1016/j.saa.2005.10.034

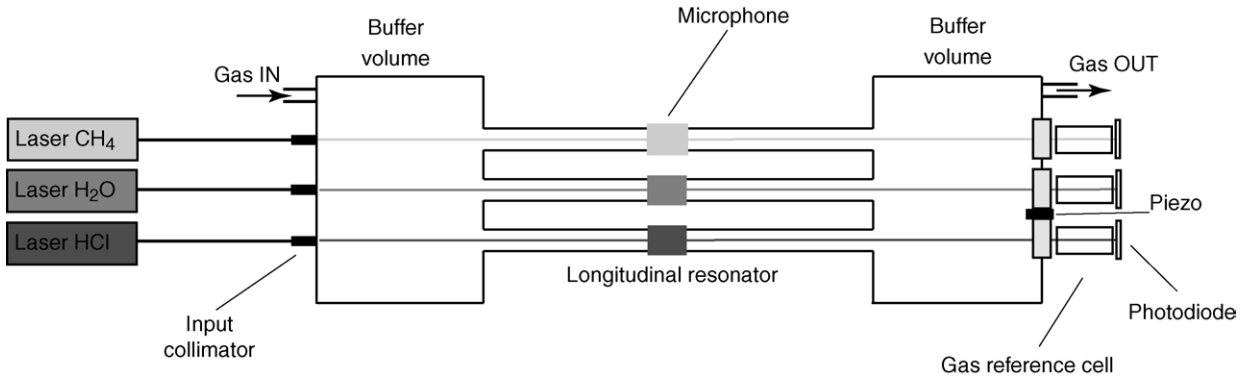

Fig. 1. Schematic view of the experimental set-up used for the measurement of CH_4, H_2O and HCl using three near-infrared DFB lasers and a PA cell including three resonators operated in their first longitudinal mode. Lasers for CH_4, H_2O and HCl are fibre-coupled and their emission is directly launched into the PA cell using a fibre collimator. Gas reference cells and a piezo transducer allow the stabilization of the laser wavelength and the tracking of the resonance frequency, respectively.

be performed in presence of O_2 and He, as these pure gases are used as carrier gases in the process.

In this paper, we describe the design of our multi-gas PA sensor based on a longitudinal acoustic resonator. The modulation scheme of the laser injection current is discussed as well as the importance of a proper calibration of the system. Finally, trace gas measurements for H_2O at 1368.6 nm, CH_4 at 1651.0 nm and HCl at 1737.9 nm are presented.

2. Experiments

2.1. Set-up

The H_2O, HCl and CH_4 detection is performed using a fibre-coupled multi-gas PA cell, made of three identical stainless steal gold-coated cylinders of 3 mm inner radius and 17 cm long, terminated by two large diameter buffer volumes (see Fig. 1). The acoustic wave is efficiently reflected at the opened ends of the small radius cylinder as a result of the large acoustic impedance mismatch with the large buffer volumes. The length of the buffer volumes was designed to realize altogether a large impedance difference and an efficient acoustic notch filtering corresponding to a quarter wavelength of the resonator standing wave (L_{buff} = 85 mm). The diameter of these volumes was optimized (d = 50 mm) to enable the implementation on the outer flange of all required elements, such as windows, loudspeaker and gas inlets. Three independent resonators have been used, each of them being excited by a DFB laser, in order to benefit from the full optical power from each laser to get the best sensitivity. A gold coating was deposited on the internal surface of the cell [5] to reduce adsorption–desorption processes inside the cell. All dimensions were optimized for high sensitivity and good immunity to environmental noise [6]. The resonators are operated in their first longitudinal mode at a resonance frequency close to 1 kHz in air. Sensitive electret microphones (Knowles EK-3132) were placed in the centre of each resonator, where the maximum of the acoustic standing wave is located. The PA signal was amplified by a low noise pre-amplifier (gain G = 100) and measured using a lock-in amplifier with a time constant usually set to 10 s. Three optical fibres terminated by a built-in collimator were fixed at the outer flange of the buffer volume. A fine mechanical alignment of the collimators allows the beams to pass through the resonators without touching the walls to avoid any wall noise. A piezo-electric transducer, fixed on the outer flange of the second volume, has been used as a sound emitter for automatic tracking of the resonance frequency (see details in Section 2.2).

The use of three fibre-pigtailed laser diodes allows easy connections to the collimators and results in much facilitated alignment procedure. The characteristics of the different lasers used for the detection of methane, water vapour and hydrogen chloride are summarized in Table 1. The reported tuning spectral range was obtained by varying the laser temperature from 5 to 40 °C. The temperature and current tuning coefficients were determined using a wavemeter and the average optical power in our experimental conditions has also been measured. Intensity modulation (IM) or wavelength modulation (WM) may be obtained by modulating the injection current of the laser, depending on the modulation conditions [7]. In our case WM was applied since it has produced a slightly higher signal than IM (25% in the case of CH_4 [8]). The modulation frequency was set to the peak of the first longitudinal mode of the acous-

Table 1
Lasers characteristics used in the experimental set-up

Gas	Wavelength (nm)	Spectral range (nm)	Temperature tuning coefficient (GHz/°C)	Current tuning coefficient (GHz/mA)	Average power (mW)
CH_4	1651.0	1649–1653	−12.6	−0.81	18
H_2O	1368.6	1368–1371	−15.8	−0.72	22
HCl	1737.9	1735–1739	−12.5	−0.86	16

tic resonator. A reference cell filled with a high concentration of the target gas at reduced pressure was placed at the exit of the cell after each resonator. The transmitted power was monitored by a photodiode. The combination of these two elements allows altogether to frequency-stabilize the laser to the target absorption line and to normalise the PA signal in case of power fluctuations.

Four mass flow controllers (MKS 1179, 2×100 sccm, 1×500 sccm and 1×1000 sccm) and a central multi-gas control unit (MKS 647C) were used to dilute gases from certified cylinders. Different buffer gases and various concentrations of HCl, H_2O and CH_4 were generated by a software control of the central multi-gas control unit. A total flow rate up to 1000 sccm was used, which resulted in a fast response time without adding any supplementary acoustic noise.

A typical resonance obtained in the tubes is shown in Fig. 2a. The frequency, half-width and quality factor of the resonance have been determined by extracting parameters from a Lorentzian fit. The response time of the cell to a concentration change has been measured and is presented in Fig. 2b. An exponential fit was used to precisely determine the time decay constant. By considering 95% of gas renewal ($1 - 1/e^3$), the response time is equal to 26 s.

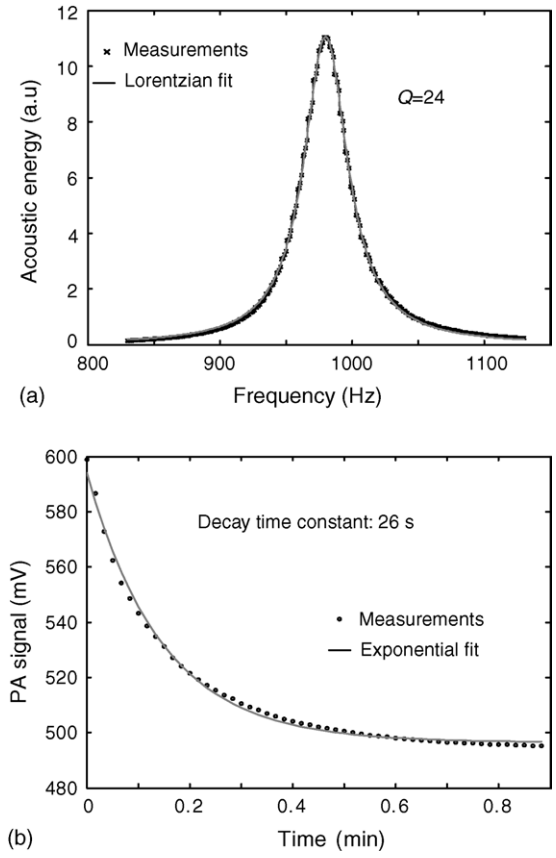

Fig. 2. (a) First longitudinal resonance showing an enhancement factor $Q = 24$. Circles are experimental points and the curve is the result of a fit by a Lorentzian distribution. (b) Response time of the PA cell to a change of methane concentration. Circles are experimental points and the curve is the result of a fit by an exponential distribution. A response time of 26 s corresponding to 95% of gas renewal is obtained.

2.2. Resonance frequency tracking

A tracking of the acoustic resonance frequency is required for automatic and long time measurements. The frequency is directly dependant on the sound velocity (C_s), which depends on temperature (T), molar mass of the gas (M) and ratio of the specific heat capacities at constant pressure and constant volume (γ):

$$f_{res} = C_s \frac{1}{2L_{eff}} = \sqrt{\frac{\gamma RT}{M}} \frac{1}{2L_{eff}} \quad (1)$$

where L_{eff} is an effective length [9] which takes into consideration boundary effects at the resonator ends and R is the perfect gas constant.

The amplitude of the PA signal rapidly decreases when the measurement frequency is shifted by a few Hertz off the resonance. Near the resonance frequency ($f = f_{res}(1 + \delta)$, $\delta \ll 1$), the amplitude of the PA signal is given by [10]:

$$\left| \frac{A(f)}{A(f_{res})} \right| \cong [1 + Q^2(1 - (1 + \delta)^2)^2]^{-1/2} \quad (2)$$

where A is the amplitude of the PA signal and Q the quality factor.

In our conditions, a frequency change of 10 Hz produces a reduction of the PA signal of 10%. Variations of tens of Hertz are typical when the buffer gas is changed. A temperature variation of 5 °C at room temperature results in a frequency shift of 8.5 Hz, producing a signal loss of 7.5%.

In order to secure a long-term operation at the correct frequency, an active stabilization of the resonance frequency has been implemented with a piezo-electric transducer used as a speaker. The tracking is usually achieved by monitoring the response in another mode of the PA cell, since the ratio of eigenmode frequencies of two modes is constant [11] for a fixed PA cell geometry (see Fig. 3). In our case it was more convenient to use the first longitudinal mode of the second buffer volume for this tracking. An electronic circuit maximizes the acoustic signal detected by the microphone and records the corresponding reference frequency. The measurement frequency (f_{meas}) is then obtained by multiplying the tracking

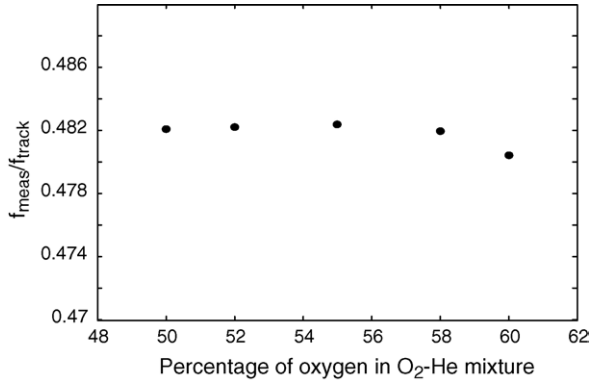

Fig. 3. Ratio of the measurement frequency (f_{meas}) and the tracking frequency (f_{track}) for different oxygen concentrations in a He–O_2 gas mixture. The photoacoustic signal was recorded using a 50 ppm CH_4 concentration.

frequency (f_{track}) by the constant ratio of the two eigenfrequencies.

2.3. Influence of the buffer gas

As PAS is an indirect method where the optical absorbed energy is not directly measured but determined through the acoustic wave generated in the sample, a proper calibration of the system is required. In optical fibre manufacturing, oxygen and helium are used as carrier gases in the process, which implies that traces measurements of hydrogenated compounds, need to be carried out in this particular gas mixture. The buffer gas has a strong influence on the sound velocity, which depends on the molar mass of the gas. Some other physical parameters (density, thermal conductivity, specific heat and viscosity) turn out to be also very different between these two carrier gases and affect the quality factor or the cell constant. In addition, the buffer gas may also influence the width of the analysed absorption line and thus modify the absorption coefficient.

The effect of the buffer gas on the PA signal has been experimentally studied with our set-up. O_2, He and N_2 were used in different dilutions with several CH_4 concentrations. Three carrier gases were obtained using mass flow controllers: 100% N_2, 50% O_2–50% He and 90% O_2–10% He with a constant flow of 500 sccm. Methane was provided in a certified gas mixture of 5000 ppm in N_2, which means that a residual of 1% or less of nitrogen was still present in the O_2–He mixtures for CH_4 concentration below 50 ppm. The response of the sensor to methane concentration is presented in Fig. 4a. Fig. 4b shows the effect of the buffer gas on the PA signal. The PA signal is 30% lower in the 50% O_2–50% He mixture than in pure N_2. This is due to the higher resonance frequency (around 1300 Hz) induced by the faster acoustic velocity in He and some other physico-thermal constant of the gas. In the 90% O_2–10% He mixture, the PA signal is reduced by a factor two. The main reason for this is due to molecular relaxation process of methane in presence of large amount of oxygen [12].

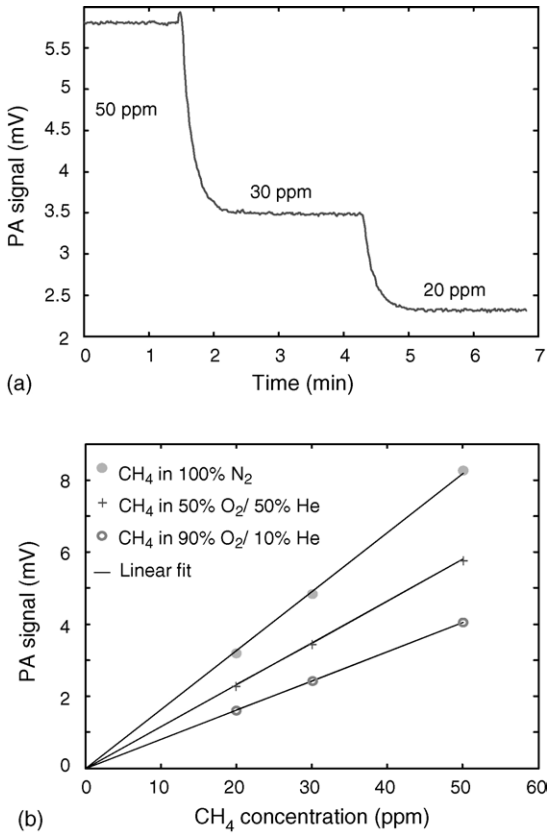

Fig. 4. (a) Typical response of the sensor to methane concentration in a 50% O_2–50% He buffer gas mixture with an integration time of 1 s. (b) Calibration curves in 100% N_2, 50% O_2–50% He and 90% O_2–10% He. Circles are experimental points and lines are linear fits.

2.4. Trace gas detection

In order to characterize our PA sensor, the detection limit for the three hydrogenated compounds was determined. The detection limit was defined for a signal-to-noise ratio (SNR) of 3. The noise was measured when purging the cell with pure N_2 (500 sccm flow rate). In addition, the wavelength of the laser was tuned slightly off the absorption line to make sure that no residual of the species contributed to the signal, especially when using polar molecules that were difficult to fully evacuate due to their sticky nature, such as H_2O and HCl. Noise measurements were made with 10 s integration time and an average value was determined for a 10 min measurement. As WM in combination with relatively low optical power was used, no window noise contribution was observed. The ambient acoustic noise was efficiently attenuated by the use of a 20 mm thick wooden enclosing box and the cell was isolated from mechanical vibrations by silent blocks.

The PA signal was measured in a specific buffer gas with different concentrations obtained by dilution of certified mixtures of methane, hydrogen chloride and water vapour using mass flow controllers. A linear fit was applied to obtain the sensitivity of the system for each gas.

Multi-gas sensing was obtained by temporal multiplexing. Each substance has been separately measured during a few minutes before the next was investigated. The simultaneous measurement of the three species was not possible due to crosstalk between the distinct resonating tubes (Fig. 5). The frequency was scanned in the three resonators while keeping the laser one on and the two others off. A crosstalk signal of 17% in tube 2 and 12% in tube 3 with respect to the total PA signal in tube 1 has been observed. However, simultaneous detection of the three gases is not required for the optical fibre manufacturing process, since only very slow variations of concentration are expected and long integration time are used (up to 30 s).

Preliminary measurements of the sensor response to methane and water vapour concentrations (Fig. 6a and b) have been made with pure N_2 as a carrier gas. Methane was measured at 1651.0 nm and water vapour at 1368.6 nm where strong overtone absorption lines take place. A linearity better than 99.9% over four orders of magnitude has been obtained for CH_4 and a linearity better than 99.9% between 1 and 50 ppm of H_2O has been achieved. A detection limit of 80 ppb of CH_4 and 24 ppb

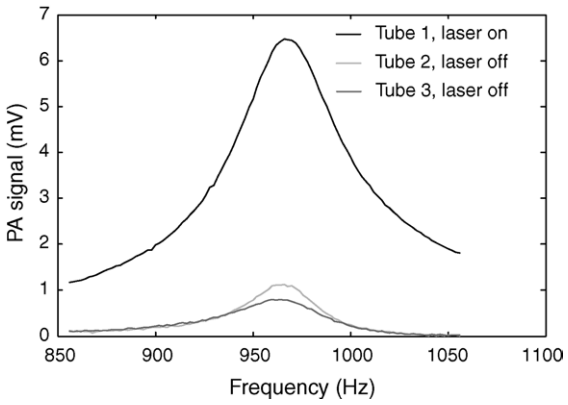

Fig. 5. Crosstalk between the three resonators. The PA signal of 100 ppm of CH_4 is recorded in tube 1, while the other two lasers in tubes 2 and 3 are switched off.

of H_2O have been extrapolated by considering a SNR = 3. In the case of water vapour, this limit has not been experimentally reached yet due to the sticky nature of water molecules and the high concentration of water vapour present in ambient air, which makes very difficult to achieve such a low H_2O concentration.

Hydrogen chloride measurements have been performed in conditions close to those experienced in optical fibre manufacturing (50% O_2–50% He), since HCl was provided in a

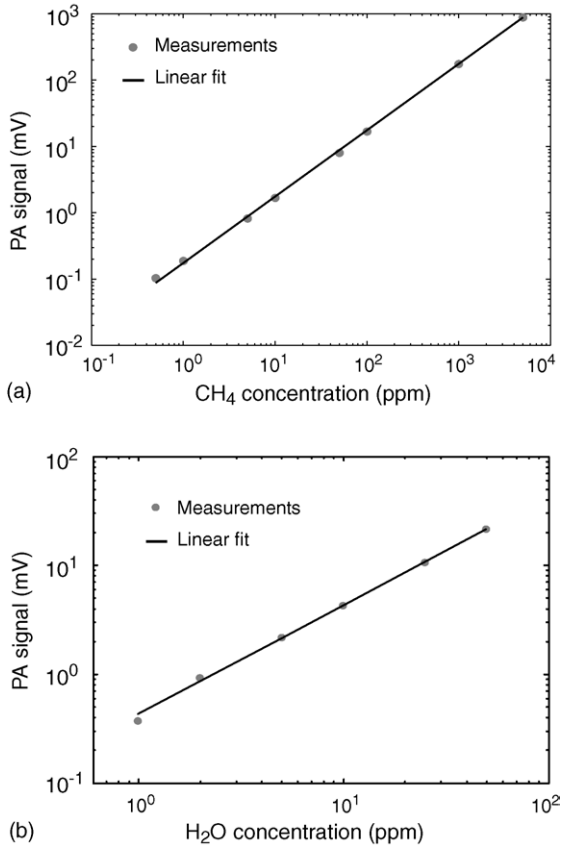

Fig. 6. Sensor sensitivity to (a) methane concentrations in pure nitrogen and (b) water vapour concentrations in pure nitrogen.

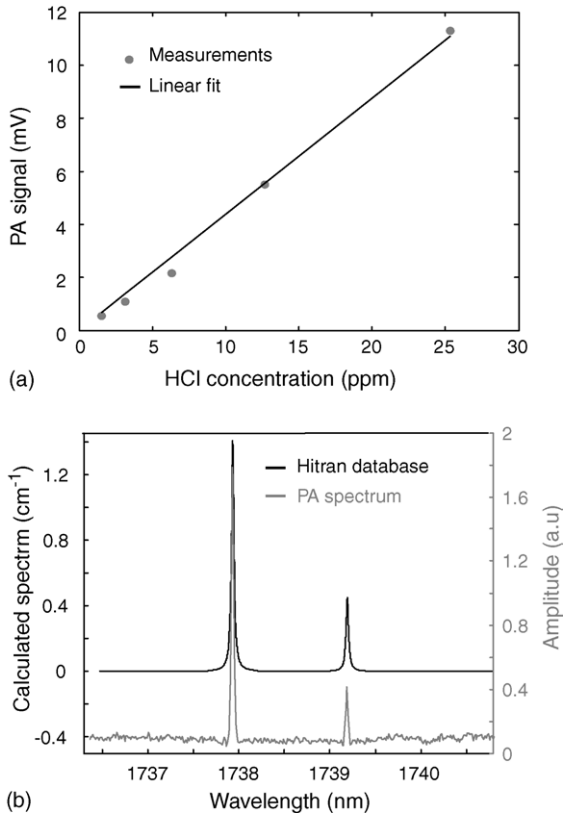

Fig. 7. (a) Sensor sensitivity to hydrogen chloride in a gas mixture of 50% O_2–50% He. (b) HCl spectrum measured using the sensor. The grey curve is the experimental data and the black line represents the corresponding absorption spectrum calculated from the Hitran database.

50 ppm cylinder diluted in helium. Several concentrations of HCl in a constant buffer gas mixture have been obtained by dilution using mass flow controllers. Results are presented in Fig. 7a. A linearity of 99.4% has been obtained between 0.5 and 25 ppm. For low concentrations, a weak quadratic dependence occurs, probably due to relaxation effects, which have to be investigated more in details. A detection limit of 30 ppb has been extrapolated when considering a linear dependence of the signal. The spectrum of this species has been measured by tuning the temperature of the laser and by recording the PA signal. A comparison between the experimental spectrum and Hitran database [13] is presented in Fig. 7b, which shows a good agreement.

All experimental results including absorption coefficients, buffer gases and detection limits, are summarized in Table 2.

Table 2
Performance of the multi-gas PA sensor

Gas	Wavelength (nm)	Absorption coefficient (cm^{-1})	Buffer gas	Detection limit (ppb)
CH_4	1651.0	0.44	N_2	80
H_2O	1368.6	1.4	N_2	24
HCl	1737.9	1.72	50% O_2–50% He	30

The absorption coefficient is calculated for pure gases and the detection limit is defined for an SNR = 3.

3. Conclusion

A multi-gas photoacoustic sensor with sub-ppm detection limit has been demonstrated. The use of a resonant configuration based on the first longitudinal mode has produced an acoustic amplification of the signal by a factor of 24. An active tracking of the resonance frequency using a servo electronics has been developed to allow long time measurements without further adjustments. The stabilization of the laser wavelength has been realized with gas reference cells fixed at the output of the PA cell. The importance of an appropriate calibration of the system has been discussed and demonstrated experimentally with nitrogen, oxygen and helium. Additional investigations to understand molecular relaxation processes for HCl are currently in progress. Trace gas measurements of hydrogen chloride, methane and water vapour in the NIR have been achieved with detection limit of 30 ppb at 1737.9 nm, 80 ppb at 1651.0 nm and 24 ppb at 1368.6 nm, respectively. Improvement of the sensor detection limit towards ppb level is an important issue and has to be considered for further developments. This can be certainly achieved in a near future using higher power or amplifier-boosted laser diodes.

Such a system demonstrates that laser spectroscopy using near-infrared laser diodes and photoacoustic detection is an efficient tool for sub-ppm detection and can be readily used for the optimization of high purity manufacturing processes. The key advantages of the system are its reliability and compactness when compared to other techniques.

Acknowledgments

The authors would like to acknowledge the Commission of Technology and Innovation (CTI) of the Swiss Government for the financial support and companies Omnisens SA and Daetwyler Fibre Optics SA for their technical and financial contributions. The authors are also grateful to NTT Electronics Corporation for providing DFB lasers.

References

[1] R.A. Rooth, A.J.L. Verhage, L.W. Wouters, Appl. Opt. 29 (25) (2001) 3643–3653.
[2] M.W. Sigrist, Rev. Sci. Instrum. 74 (1) (2003) 486–490.
[3] L. Menzel, A.A. Kosterev, R.F. Curl, F.K. Tittel, C. Gmachl, F. Capasso, D.L. Sivco, J.N. Baillargeon, A.L. Hutchinson, A.Y. Cho, W. Urban, Appl. Phys. B 72 (2001) 859–863.
[4] K. Kincade, Laser Focus World 39 (3) (2003) 97.
[5] S.M. Beck, Appl. Phys. 24 (1985) 1761–1763.
[6] J.-Ph. Besson, S. Schilt, L. Thévenaz, Spectrochim. Acta A 60 (14) (2004) 3449–3456.
[7] S. Schilt, L. Thévenaz, Infrared Phys. Technol., in press.
[8] S. Schilt, J.-Ph. Besson, L. Thévenaz, in: J.M. Lopez-Higuera, B. Culshaw (Eds.), Proceedings of the Second European Workshop on Optical Fiber Sensors, SPIE vol. 5502, Bellingham, Washington, 2004, pp. 317–320.
[9] L.E. Kinsler, A.R. Frey, A.B. Coppens, J.V. Sanders, Fundamentals of Acoustics, Wiley, New York, 2001.
[10] C.F. Dewey, in: Y.-H. Pao (Ed.), Optoacoustic Spectroscopy and Detection, Academic Press, New York, 1977, pp. 47–77 (Chapter 3).
[11] G. Angeli, Z. Bozoki, A. Miklos, A. Lörincz, A. Thöny, M. Sigrist, Rev. Sci. Instrum. 62 (3) (1990) 810–813.
[12] S. Schilt, J.-Ph. Besson, L. Tévenaz, J. de Phys. IV 125 (2005) 7–10.
[13] L.S. Rothman, D. Jacquemart, A. Barbe, D. Chris Benner, M. Birk, L.R. Brown, M.R. Carleer, C. Chackerian Jr., K. Chance, et al., J. Quant. Spectrosc. Radiat. Transfer 96 (2) (2005) 139–204.